Zero-range Fermi gas along the BCS-BEC crossover

Renato Pessoa,[1,*] S. A. Vitiello,[2,3] and K. E. Schmidt[4,2]

[1]*Instituto de Física, Universidade Federal de Goiás, 74001-970 Goiânia, Goias, Brazil*

[2]*Instituto de Física Gleb Wataghin, Universidade Estadual de Campinas, 13083-970 Campinas, São Paulo, Brazil*

[3]*CENAPAD-SP, University of Campinas, 13083-889 Campinas, São Paulo, Brazil*

[4]*Department of Physics, Arizona State University, Tempe, Arizona 85287, USA*

(Received 7 June 2019; published 4 November 2019)

Properties of the ground state of an unpolarized ultracold Fermi gas along the BCS-BEC crossover are investigated by the variational and diffusion Monte Carlo methods. We apply the Wigner-Bethe-Peierls boundary condition in our calculations to avoid any bias from using an interatomic potential with finite effective range. Properties for several values of the scattering length are studied in the range $-8 \leqslant 1/ak_F \leqslant 4$, including the unitary limit. The contact parameters as a function of scattering length are obtained by fitting the pair distribution functions for particles with different spins. The energies and contact parameters are in very good agreement with experimental data reported in the literature.

DOI: 10.1103/PhysRevA.100.053601

I. INTRODUCTION

Ultracold gases, because of their fantastic tunability, allow one to go from the weak interaction regime to the strong one. They are of interest by themselves and because it is possible to use them to simulate condensed-matter systems [1]. An important achievement in the research on ultracold Fermi gases was the investigation of the crossover of a Bose-Einstein condensate (BEC) to a Bardeen-Cooper-Schrieffer (BCS) superfluid; for a review, see Ref. [2]. These are dilute systems and their interaction potential ranges are negligible compared to the mean distance between particles and to the thermal de Broglie wavelength. Thus these systems have predominantly two-body interactions that can be described through collisions between the atoms. The dominant effect in the collision dynamics is a single s-wave partial-wave scattering. This is because relative momenta of particles are small and, as is shown by the effective range theory, collisions are completely determined by the s-wave scattering for fermionic unpolarized systems in the ultracold regime. The interactions at this low-energy limit can be described by a single parameter, the scattering length. This situation allows the replacement of the true interatomic potential by a simpler one, as long as it is adjusted to reproduce a given value of the scattering length.

Until recently, theoretical studies were performed with pseudopotentials [3] for the contact interaction or finite-range potentials extrapolated to zero range, to avoid dealing with an ill-behaved wave function in this limit [3–9]. A series of calculations to perform the extrapolation to a zero-range limit is not the only inconvenience of this approach. Uncertainties about the influence of the true ground state of the chosen potential are among the difficulties of this approach. In a previous work, we showed that a contact or zero-range potential can be used in Monte Carlo calculations [10] to investigate the properties of an unpolarized, ultracold Fermi gas in the unitary limit where the scattering length $a \to \pm\infty$.

In this paper, we use a zero-range potential to investigate the equation of state of an ultracold Fermi gas in the BCS-BEC crossover. We have also obtained the radial distribution functions of unlike spins and the contact parameter per unit volume for several values of the scattering length a in the range $-8 < 1/ak_F < 4$, where k_F is the Fermi wave vector. The fitting of the radial distribution functions for different values of ak_F provides the contact parameters.

II. METHODOLOGY

To treat the system of N unpolarized, ultracold Fermi atoms, we consider a zero-range potential and apply the Wigner-Bethe-Peierls boundary condition method [11], where the boundary condition for the wave function at the center of the well replaces the Schrödinger equation solution. The boundary condition satisfied by particle pairs of the wave function in the limit of very weak interactions is given by

$$\psi(r_{ij'} \to 0) \propto \frac{1}{r_{ij'}} - \frac{1}{a}, \tag{1}$$

when the $r_{ij'} = |\mathbf{r}_i - \mathbf{r}_{j'}|$ are smaller than a cutoff. We denote up-spin (down-spin) particles with unprimed (primed) coordinates. Other pairs are treated as satisfying the free Schrödinger equation

$$-\frac{\hbar^2}{2m}\sum_i^N \nabla_i^2 \psi(R) = E\psi(R) \tag{2}$$

where $R \equiv \{\mathbf{r}_1, \mathbf{r}_{1'}, \ldots, \mathbf{r}_{N/2}, \mathbf{r}_{N'/2}\}$.

The Wigner-Bethe-Peierls boundary condition of Eq. (1) has a universal form for short-range potentials. These potentials are characterized by the property that beyond a certain radius of action (or range) r_0 they can be neglected.

*rpessoa@ufg.br

Qualitatively, this condition is met at distances $r \gg r_0$ if the confinement kinetic energy inside a sphere of radius r is much larger than the absolute value of the potential energy outside it.

The wave-function model used to describe the system must be antisymmetric and it is given by

$$\Psi_T(R) = \prod_{ij'} f(r_{ij'})\Phi_{\rm BCS}, \tag{3}$$

$$\Phi_{\rm BCS} = \mathcal{A}[\phi(\mathbf{r}_{11'})\phi(\mathbf{r}_{22'})\cdots\phi(\mathbf{r}_{N/2\,N'/2})] \tag{4}$$

where $f(r)$ is a factor of the Jastrow form that correlates only up-down spin pairs. The BCS function $\Phi_{\rm BCS}$ takes into account the antisymmetrical character of the system's fermionic wave function. The operator $\mathcal{A}$ antisymmetrizes particles with the same spin and $\phi(r)$ describes the Cooper-pair orbital the general form of which is

$$\phi(r) = \sum_{j}^{N_s} \alpha_j \exp(i\mathbf{k}_j \cdot \mathbf{r}), \tag{5}$$

where $\{\alpha_j\}$ are variational parameters associated with the different N_s shells with momenta $\mathbf{k}_j = \frac{2\pi}{L}(n_x, n_y, n_z)$. The BCS part of the wave function in Eq. (3) reduces to a product of two Slater determinants if the number of shells is such that the maximum value of the vector wavelength is $k_{\rm max} = k_F$ [8,12–14]. The number of shells is increased until variational energy has converged. Most of the calculations for the scattering length values considered in this paper used $N_s = 20$, the same number of shells used in the unitary regime of our previous work [10]. However, we used $N_s = 10$ for $-1.0 < ak_F < 0$ and $0 < ak_F \leqslant 0.75$ corresponding to the BCS and the BEC regions, respectively.

The computational simulation starts with the variational minimization of the expectation value of the Hamiltonian:

$$E_{\rm VMC} = \frac{\langle\Psi_T|H|\Psi_T\rangle}{\langle\Psi_T|\Psi_T\rangle}. \tag{6}$$

The variational principle ensures that this energy is an upper bound of the exact ground-state energy. The set of parameters to be optimized consists of those in the Jastrow term and the coefficients of the shells $\{\alpha\}$. The stochastic reconfiguration method [15] is employed to optimize the set of shell parameters for each value of the scattering length. By sampling a set of configurations distributed in accordance with the probability density obtained from $|\Psi_T|^2$, the energy of Eq. (6) is estimated through the average of the local energy:

$$E_L = \left\langle \frac{H\Psi_T}{\Psi_T} \right\rangle. \tag{7}$$

The Metropolis algorithm [16] is used in the sampling process. However, because of the Wigner-Bethe-Peierls boundary condition, and the form of the trial wave function, the local energy of the system diverges when the distance between two particles with different spins goes to zero. Those divergences are integrable and handled numerically by inserting one more move in the standard Monte Carlo sweep [10,14]. After an attempt to move the N particles, the particle positions of the closest unlike spin pair are exchanged. The new configuration is then used in the energy calculation with the heat-bath acceptance probability. This procedure eliminates the divergences in the local energy for the scattering length range studied in this paper.

The Jastrow term in Eq. (3) is given by

$$f(r) = \begin{cases} A\left[\exp\left(-\frac{r}{a}\right) + \cosh(\lambda r) - \frac{r}{a}\right]\frac{1}{r}, & 0 < ak_F < \infty, \\ B\left[\cosh(\lambda r) - \frac{r}{a}\right]\frac{1}{r}, & -\infty < ak_F < 0. \end{cases} \tag{8}$$

The constants A and B are chosen such that $f(r = D) = 1$, where D is the range of the Jastrow term, $D \leqslant \frac{L}{2}$. It is optimized to give the lowest variational energy in Eq. (6). The parameter λ is set in a way to guarantee the continuity of the wave function by making $\frac{df}{dr} = 0$ at $r = D$. For positive values of scattering length, an exponential term takes into account the bound state of the Fermi gas. Pairs typically dominate the behavior of the system when their sizes are smaller than the average distance between the particles of the gas, in other words, when $ak_F < 3.0$ [5,13]. For the range of negative scattering length, in Eq. (8), there is no bound state and the Jastrow term keeps the condition $f(r) \propto (\frac{1}{r} - \frac{1}{a})$ when $r \to 0$. In the unitary regime the Jastrow term is the same used when $a \to \pm\infty$ [10].

To go beyond the variational calculations we apply the diffusion Monte Carlo (DMC) method. In this method the Schrödinger equation is written as a diffusion equation:

$$-\frac{\partial\psi(R;\tau)}{\partial\tau} = (H - E_0)\psi(R;\tau), \tag{9}$$

where $\tau = it/\hbar$ is an imaginary time and E_0 is an estimation of the system ground-state energy, which is inserted in the equation to stabilize the norm of the eigenstate ψ. A typical way [17,18] of solving Eq. (9) involves writing a propagation equation:

$$\Psi_T(R)\psi(R;\tau+\Delta\tau) = \int d^3R' \frac{\Psi_T(R)}{\Psi_T(R')} G(R,R';\Delta\tau)\Psi_T(R')\psi(R',\tau), \tag{10}$$

where $G(R, R'; \Delta\tau)$ is a Green's function defined in a small time $\Delta\tau$ and Ψ_T is used as a guide function. The propagator in Eq. (10) can be rewritten in terms of the free-particle propagator [13,18]:

$$\frac{\Psi_T(R)}{\Psi_T(R')} G(R,R';\Delta\tau) = G_0(R,R')\frac{\Psi_T(R)G(R,R';\Delta\tau)}{\Psi_T(R')G_0(R,R')} \tag{11}$$

$$\approx G_0(R,R')\exp\left\{-\frac{\Delta\tau}{2}[E_L(R) + E_L(R')] - E_0\Delta\tau\right\}, \tag{12}$$

where G_0 is a propagator of free particles with a drifted term like

$$G_0(R,R') = \left[\frac{m}{2\pi\hbar^2\Delta\tau}\right]^{\frac{3N}{2}} \exp\left[-\frac{m}{2\hbar^2\Delta\tau}\left(R - R' - \frac{\hbar^2}{2m}\Delta\tau\nabla\ln[\Psi(R)]\right)^2\right] \tag{13}$$

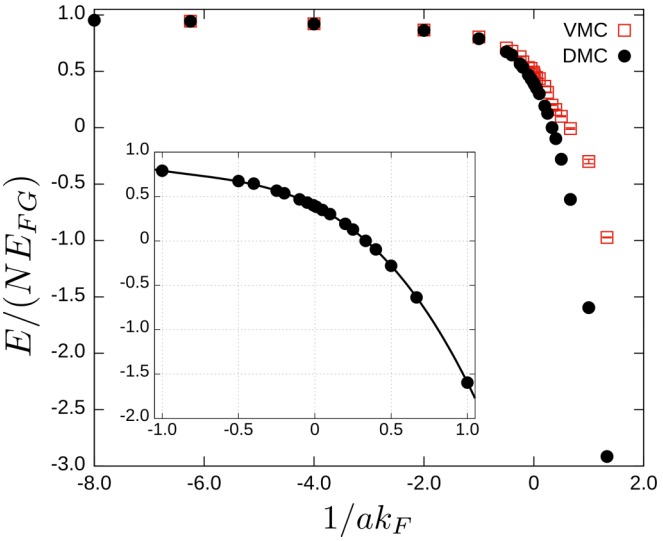

FIG. 1. Energy per particle as a function of $1/ak_F$. The inset shows the results around the unitary limit ($ak_F \to \infty$) and the line is the fit of the equation of state in Eq. (15).

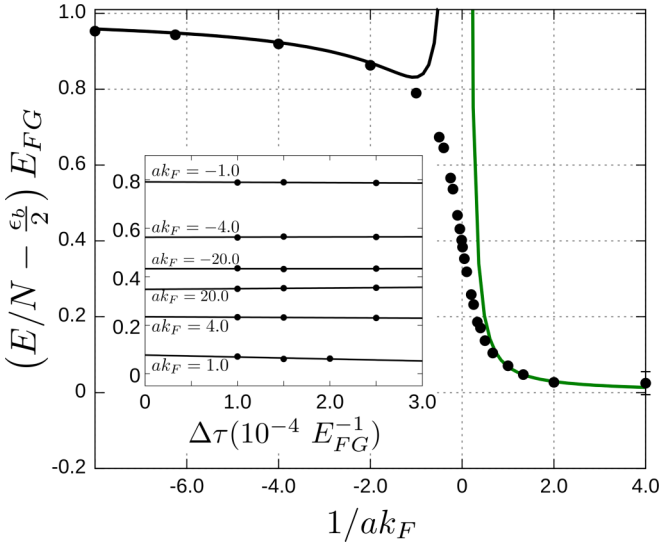

FIG. 2. Energy per particle as a function of $1/ak_F$ (see text). The green solid line is the difference of the energies obtained through the equation of state of the gas formed by pairs of unlike spin particles in the BEC limit in Eq. (16). The solid black line is the result of the BCS limit [27,28]. The inset shows energies for different values of $\Delta\tau$.

used to move the particles in the system. The short time $\Delta\tau$ is small enough to avoid divergences during the simulation, since the logarithmic term prevents an overlap in the positions of two particles with different spins. After propagating the particles through Eq. (13), the branching process of the walkers is considered with the weight given by the exponential term in Eq. (12). The fixed-node approximation is considered in this paper, that is, we assign zero weight to any walker trying to cross the nodal surface of the guiding function during the drift process. This approach avoids the typical signal problem of systems formed by fermions and provides an upper bound for the ground-state energy.

After sampling the particle positions with the propagator of Eq. (12), the DMC energy is calculated through the mixed estimator

$$E_{\rm DMC} = \frac{\langle \Psi_T | H | \psi \rangle}{\langle \Psi_T | \psi \rangle}. \tag{14}$$

Since the nodes of the wave function are fixed, Eq. (14) provides an upper bound for the eigenenergy of the system [17]. On the other hand, $E_{\rm DMC}$ goes to the exact value of the energy as $\tau \to \infty$ within a given nodal surface.

III. RESULTS AND DISCUSSION

Energies per atom as a function of $1/ak_F$ are presented in Fig. 1. The red squares represent the variational energies and the solid black circles are the DMC energies. The results are obtained from computational simulations with $N = 66$ particles inside a box with periodic boundary conditions, such that we have ensured the thermodynamic limit [19]. While both energies are very close, for $1/ak_F \ll -1.0$, the difference increases significantly as the system approaches the deep BEC region ($1/ak_F \gg 1.0$). This is an indication that the variational model gives a good description of the Fermi gas in the BCS region. The inset of Fig. 1 shows the DMC energies for the range $-1.0 < 1/ak_F < 1.0$. The equation of state near the unitary regime was fitted to the expression

$$\frac{E}{NE_{\rm FG}} = \xi - \frac{\zeta}{ak_F} - \frac{5\nu}{3(ak_F)^2} + \cdots \tag{15}$$

where $E_{\rm FG}$ is the free Fermi gas energy, ξ is the Bertsch parameter, ζ is related to the contact parameter, and ν a constant. Our fit gives $\xi = 0.394(1)$, $\zeta = 0.867(5)$, and $\nu = 0.478(2)$. The contact parameter can be obtained [5,20–22] through the derivative of the energy $\frac{d(nE/N)}{da^{-1}} = -\frac{\hbar^2 C}{4\pi m}$, where $n = \frac{k_F^3}{3\pi^2}$ is the system density. Performing the derivative of Eq. (15), the contact parameter in the unitary limit $C/k_F^4 = 2\zeta/5\pi$ is estimated as $C/k_F^4 = 0.1104(6)$. The related quantity, the contact parameter per unit of volume, is given as $\mathcal{C}/Nk_F = 3\pi^2 C/k_F^4 = 3.27(2)$. This value is bigger than our previous result obtained by fitting the unlike spin pair distribution function, 2.848(1) [10]. Nevertheless, both values are in reasonable agreement with experimental values obtained with different techniques. Hoinka *et al.* [23] used Bragg spectroscopy to obtain 3.06(8), and Sagi *et al.* [24] reported 2.9(3) by using radio-frequency spectroscopy close to the unitary regime of the gas.

The formation of bound pairs of particles with different spins can be more clearly seen if half of the pair binding energy $\frac{\epsilon_b}{2} = -\frac{\hbar^2}{2ma^2}$ is subtracted from the energy per particle displayed in Fig. 1. This was done for all positive values of the scattering length. We show these results for a DMC calculation in Fig. 2. The energy difference tends to zero when the positive scattering length decreases, indicating the formation of bound pairs of particles with different spins. This happens when the gas goes into the deep BEC regime. This shows that the formation of Fermion pairs is a dominant process when the scattering length is small enough. The pair behavior begins to manifest for $ak_F < 3.0$ when the energy per particle becomes negative. The solid green line is the

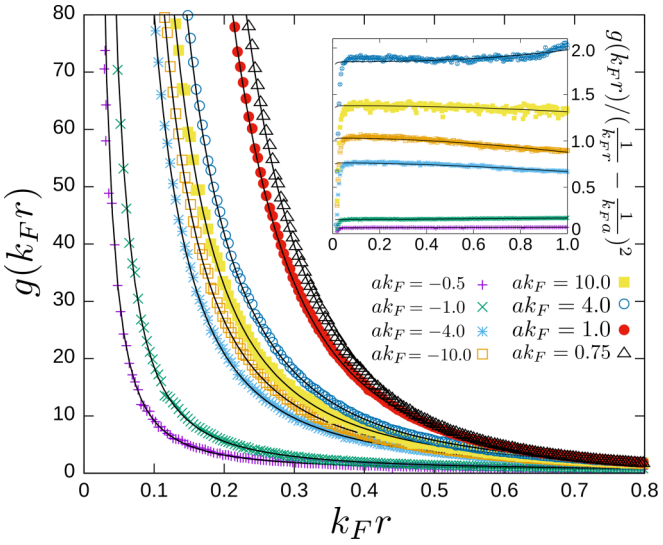

FIG. 3. The unlike spin pairs distribution function as a function of the distance. The lines are the best fits to the function $g(k_F r) = b_0 + \frac{b}{k_F r}(\frac{1}{k_F r} - \frac{2}{ak_F})$. In the inset we show $g(k_F r)/(\frac{1}{k_F r} - \frac{1}{k_F a})^2$.

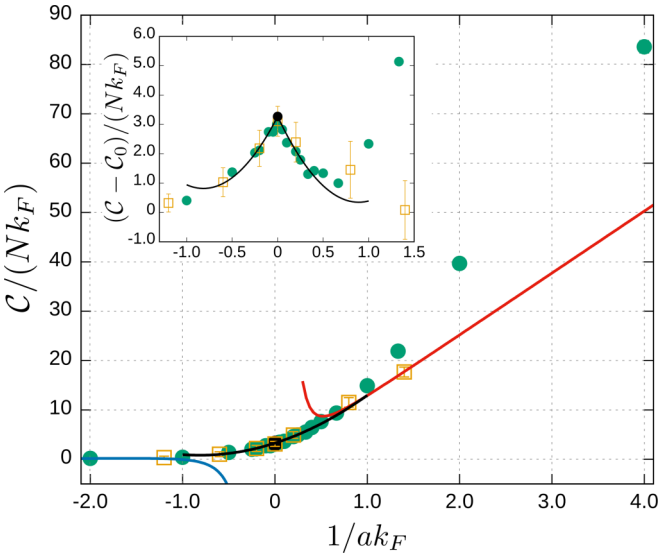

FIG. 4. Contact parameter per unit of volume as a function of $1/ak_F$ represented by green dots. The black dot is its value at the unitary limit. Empty squares are the experimental results obtained using Bragg spectroscopy [33]. The solid black line is the derivative of Eq. (15). The blue and red lines are results of BCS perturbation expansion [27,28,35] and for the BEC limit [9,12,25], respectively. The inset shows the contact parameter minus the contribution of the bound pair $\mathcal{C}_0$.

difference of energies calculated with the analytical equation of state of the gas formed by pairs of unlike spin particles in the BEC limit [9,12,25]:

$$\frac{E}{N} - \frac{\epsilon_b}{2} = \frac{5}{18\pi} k_F a_{dd} \left[1 + \frac{128}{15\sqrt{6\pi^3}} (k_F a_{dd})^{3/2}\right] E_{\rm FG}, \quad (16)$$

where $a_{dd} = 0.6a$ [26] is the dimer-dimer scattering length. The ϵ_b energy is equal to zero for negative scattering lengths and at the unitary limit because there is no molecule formation in these cases. Therefore, the values shown on the left side of Fig. 2 coincide with the energy per particle of the system. Note that the results tend to BCS perturbation expansion of a weakly attractive Fermi gas [27,28] for $1/ak_F \ll -1$; this is the region where the variational model gives a good description for the system and the variational energy is very close to the one calculated with DMC, Fig. 1. In this regime, the system promotes the formation of Cooper pairs. The inset shows for different values of τ that our results are consistent with the extrapolation $\Delta\tau \to 0$.

The unlike spin pair distribution function at short limit distances is given by $g(r) = \mathcal{A}(\frac{1}{r^2} - \frac{2}{ar} + \cdots)$ [5,21,29,30], where $\mathcal{A}$ is proportional to the contact parameter. The contact parameter C is associated with the two-particle short distance behavior [21,31,32] and can be expressed [5] as $C = 8\pi^2 n^2 \mathcal{A}$. Therefore, the pair function distribution is related to the contact parameter through

$$g(k_F r) = \frac{9\pi^2}{8} \frac{C}{k_F^4} \left[\frac{1}{(k_F r)^2} - \frac{2}{(ak_F)(k_F r)}\right] + \text{const.} \quad (17)$$

In Fig. 3, we present extrapolated results, $g(k_F r) = 2g_{\rm DMC}(k_F r) - g_{\rm VMC}(k_F r)$, for the unlike spin pair distribution functions for different values of the scattering length, where $g_{\rm DMC}$ and $g_{\rm VMC}$ are the results obtained in DMC and VMC calculations, respectively. The lines are fitted curves to the function $g(k_F r) \simeq b_0 + \frac{b}{k_F r}(\frac{1}{k_F r} - \frac{2}{ak_F})$, where b_0 and b are parameters.

The contact parameter per unit of volume $\mathcal{C}/Nk_F = 8b/3$ is obtained by considering the parameter b of the fitted curves to $g(k_F r)$ for each value of the scattering length in this paper. The contact parameter per unit of volume as a function of $1/ak_F$ is represented by green dots in Fig. 4. At the unitary limit, its value is depicted by a black dot. The black line is the derivative of Eq. (15) as a function of $-1/a$ The blue and red lines are the derivatives of fitted curves shown in Fig. 2 for BCS and BEC limits, respectively. Our quantum Monte Carlo results are in very good agreement with the experimental values obtained using Bragg spectroscopy [33]. The inset of Fig. 4 shows the results for the contact parameters per unit of volume minus the contribution of the bound pair $\mathcal{C}_0/(Nk_F) = 3\pi^2 C_0/k_F^4$, where $\frac{d(n\epsilon_b/2)}{da^{-1}} = -\frac{\hbar^2 C_0}{4\pi m}$, a contribution which is zero for negative scattering lengths [22,34]. Our variational results (not shown in the figure) are very close to those of the extrapolated calculations for negative scattering lengths. This is the same behavior observed for the results of the energy. It is a further indication that our variational model gives a better Fermi gas description near the BCS regime than in the BEC regime, where pairs are formed by unlike spin particles.

IV. SUMMARY

We performed Monte Carlo simulations of an ultracold Fermi gas with a contact interaction and finite scattering lengths. The Wigner-Bethe-Peierls boundary condition is considered in the calculations. Our variational wave function

gives a good description of the system in the BCS region for $1/ak_F \ll -1$. Over the whole BCS-BEC crossover, our results for the radial distribution of pairs $g(k_F r)$ and the contact parameters, as a function of the scattering length, are in very good agreement with experimental results obtained via Bragg spectroscopy. Moreover, since we use a zero-range potential as more than just a proof of principle, our calculations produce results free from any bias arising from extrapolations of a given potential to the zero-range limit.

ACKNOWLEDGMENTS

The authors acknowledge financial support from the Brazilian agencies Fundação de Amparo à Pesquisa do Estado de São Paulo project (Proc. No. 2016/17612-7). Part of the computations was performed at the Centro Nacional de Processamento de Alto Desempenho em São Paulo. R.P. acknowledges the Fundação de Amparo à Pesquisa do Estado de Goiás and the computer resources of the Laboratório de Computação Científica - Universidade Federal de Goiás. K.E.S. was supported by NSF Grant No. PHY-1404405.

[1] C. Gross and I. Bloch, Science **357**, 995 (2017).
[2] G. C. Strinati, P. Pieri, G. Röpke, P. Schuck, and M. Urban, Phys. Rep. **738**, 1 (2018).
[3] P. O. Bugnion, P. López Ríos, R. J. Needs, and G. J. Conduit, Phys. Rev. A **90**, 033626 (2014).
[4] X. Li, J. Kolorenč, and L. Mitas, Phys. Rev. A **84**, 023615 (2011).
[5] S. Gandolfi, K. E. Schmidt, and J. Carlson, Phys. Rev. A **83**, 041601(R) (2011).
[6] J. Carlson, S. Gandolfi, K. E. Schmidt, and S. Zhang, Phys. Rev. A **84**, 061602(R) (2011).
[7] Michael McNeil Forbes, S. Gandolfi, and A. Gezerlis, Phys. Rev. A **86**, 053603 (2012).
[8] J. Carlson, S.-Y. Chang, V. R. Pandharipande, and K. E. Schmidt, Phys. Rev. Lett. **91**, 050401 (2003).
[9] G. E. Astrakharchik, J. Boronat, J. Casulleras, and S. Giorgini, Phys. Rev. Lett. **93**, 200404 (2004).
[10] R. Pessoa, S. Gandolfi, S. A. Vitiello, and K. E. Schmidt, Phys. Rev. A **92**, 063625 (2015).
[11] H. Bethe and R. Peierls, Proc. R. Soc. A **148**, 146 (1935).
[12] S. Giorgini, L. P. Pitaevskii, and S. Stringari, Rev. Mod. Phys. **80**, 1215 (2008).
[13] S. Y. Chang, V. R. Pandharipande, J. Carlson, and K. E. Schmidt, Phys. Rev. A **70**, 043602 (2004).
[14] R. Pessoa, S. A. Vitiello, and K. E. Schmidt, J. Low Temp. Phys. **180**, 168 (2015).
[15] S. Sorella, Phys. Rev. B **64**, 024512 (2001).
[16] N. Metropolis, A. W. Rosenbluth, M. N. Rosenbluth, A. H. Teller, and E. Teller, J. Chem. Phys. **21**, 1087 (1953).
[17] P. J. Reynolds, D. M. Ceperley, B. J. Alder, and W. A. Lester, J. Chem. Phys. **77**, 5593 (1982).
[18] W. A. Lester and B. L. Hammond, Annu. Rev. Phys. Chem. **41**, 283 (1990).
[19] M. M. Forbes, S. Gandolfi, and A. Gezerlis, Phys. Rev. Lett. **106**, 235303 (2011).
[20] E. Braaten and L. Platter, Phys. Rev. Lett. **100**, 205301 (2008).
[21] S. Tan, Ann. Phys. (NY) **323**, 2971 (2008).
[22] F. Werner and Y. Castin, Phys. Rev. A **86**, 013626 (2012).
[23] S. Hoinka, M. Lingham, K. Fenech, H. Hu, C. J. Vale, J. E. Drut, and S. Gandolfi, Phys. Rev. Lett. **110**, 055305 (2013).
[24] Y. Sagi, T. E. Drake, R. Paudel, R. Chapurin, and D. S. Jin, Phys. Rev. Lett. **114**, 075301 (2015).
[25] T. D. Lee, K. Huang, and C. N. Yang, Phys. Rev. **106**, 1135 (1957).
[26] D. S. Petrov, C. Salomon, and G. V. Shlyapnikov, Phys. Rev. Lett. **93**, 090404 (2004).
[27] K. Huang and C. N. Yang, Phys. Rev. **105**, 767 (1957).
[28] T. D. Lee and C. N. Yang, Phys. Rev. **105**, 1119 (1957).
[29] J. Hofmann and W. Zwerger, Phys. Rev. X **7**, 011022 (2017).
[30] W. Zwerger, arXiv:1608.00457v1.
[31] S. Tan, Ann. Phys. (NY) **323**, 2952 (2008).
[32] S. Tan, Ann. Phys. (NY) **323**, 2987 (2008).
[33] E. D. Kuhnle, S. Hoinka, H. Hu, P. Dyke, P. Hannaford, and C. J. Vale, New J. Phys. **13**, 055010 (2011).
[34] G. Bertaina and S. Giorgini, Phys. Rev. Lett. **106**, 110403 (2011).
[35] F. Werner, L. Tarruell, and Y. Castin, Eur. Phys. J. B **68**, 401 (2009).